Hsiung *et al.*
Progress in Earth and Planetary Science (2025) 12:4
https://doi.org/10.1186/s40645-024-00675-2

Progress in Earth and Planetary Science

RESEARCH ARTICLE

Open Access

Reconstruction of bottom water ventilation changes in the West Philippine Sea during the last glacial-interglacial period

Wei-Cheng Hsiung[1,2], Yuan-Pin Chang[2,3*], Horng-Sheng Mii[4], Ken Ikehara[5], Toshiya Kanamatsu[6] and Hui-Ling Lin[2]

Abstract

Global deep-water circulation plays a crucial role in regulating long-term carbon storage in both the ocean and atmosphere. During the last glacial period, it is reported that this circulation slowed down, causing glacial intermediate water to descend to depths of 2,000 m in the Pacific. This process is thought to be a key mechanism in restricting global deep-water circulation and reducing atmospheric carbon dioxide concentrations during glacial periods. Conversely, the emergence of a potential deep-water formation zone in the northwestern Pacific during deglaciation adds complexity to these circulation patterns. Addressing the scarcity of sedimentary records in the subtropical western Pacific for paleoceanographic reconstruction, sediment core YK15-01 PC13 (23.5°N, 124.24°E; southeast of Ishigaki Island at a depth of 2,520 m) used in this study, collected in 2015. By analyzing coexisting planktonic and benthic foraminifera, we have reconstructed radiocarbon ventilation ages in this region since the last glacial maximum. Our findings, including ventilation age records compiled from the Atlantic and Pacific Oceans, reveal opposing deep-water circulation patterns from the last glacial to the interglacial period, including during the Heinrich Event 1 (HE1) and Younger Dryas (YD). This supports the theory of a seesaw-like oscillation in ocean circulation. Furthermore, the improved ventilation observed during HE1 and YD suggests a contribution from deep water formed in the high-latitude Pacific, influenced by cooler climate conditions. This glacial North Pacific deep water, likely confined to the northwestern Pacific, has left its mark in the subtropical western Pacific records. This research enhances our understanding of deep-water circulation interactions between the Atlantic and Pacific and contributes new insights into the role of northern Pacific deep water in influencing atmospheric carbon dioxide variations during the last deglaciation.

Keywords Deep-water circulation, Intermediate water, Ventilation, Radiocarbon ages, Glacial period

*Correspondence:
Yuan-Pin Chang
yuanpin.chang@mail.nsysu.edu.tw
Full list of author information is available at the end of the article

1 Introduction

Ocean ventilation refers to the process by which water masses and dissolved substances are exchanged between the surface ocean and the subsurface or deep ocean (Khatiwala et al. 2012). Deep water is typically formed in high-latitude regions due to its higher density, resulting in less-ventilated deep water in tropical and subtropical oceans, as these areas are distant from the source regions (Talley 2013). The global deep-water circulation, also known as thermohaline circulation or the Great Ocean Conveyor, was comprehensively described by Broecker (2010). In the Great Ocean Conveyor model, the sinking of North Atlantic Deep Water (NADW) initiates the Atlantic Meridional Overturning Circulation (AMOC), playing a crucial role in driving thermohaline circulation and extending southward to the Southern Ocean. The NADW then mixes with water masses formed in the Southern Ocean, flowing eastward to the Indian Ocean. Eventually, the modified North Atlantic-sourced deep water reaches the Pacific (Broecker 2010), turns southward in the North Pacific, and returns to the Southern Ocean (Kawabe and Fujio 2010).

Deep-water circulation likely differed during the glacial period. Due to the increased ice sheet coverage in high latitudes, the formation area of North Atlantic Deep Water (NADW) shifted southward, and the intensity of deep-water sinking was weaker during the glacial period compared to the present (Sigman et al. 2010) or even transformed to a converse pattern (Negre et al. 2010). Concurrently, a ventilation boundary emerged around a water depth of 2,000 m in the North Pacific during the last glacial maximum, indicating potential deep-water or enhanced intermediate water formation in the region (Herguera et al. 1992; Keigwin 1998; Matsumoto et al. 2002). During deglaciation, the release of carbon dioxide from deep water is considered a key mechanism for the dramatic increase in atmospheric CO_2. One significant indicator of this is the decrease in atmospheric radiocarbon activity (Broecker and Barker 2007). Atmospheric radiocarbon activities reconstructed from stalagmites (Beck et al. 2001), corals (Fairbanks et al. 2005), and foraminifera (Hughen et al. 2004) all indicate higher values during the last glacial period compared to the present. However, atmospheric $\Delta^{14}C$ decreased by about 190‰ between 17.5 and 14.5 kyr BP during the last deglaciation (Broecker and Barker 2007). Although some questions remain unanswered, the most accepted explanation for the radiocarbon activity differences is the release of more radiocarbon-depleted water from the abyssal ocean reservoir formed during the last glacial (Broecker and Barker 2007). This exchange of carbon from the abyssal depths to shallower ocean layers and the atmosphere, associated with increased atmospheric carbon dioxide levels (Monnin et al. 2001), might have been facilitated by vertical mixing in the Southern Ocean (Anderson et al. 2009). Numerous studies have provided records supporting the emission of ^{14}C-depleted CO_2 during deglaciation, spanning from the Atlantic to the Southern Ocean (Skinner et al. 2010), the Eastern Equatorial Pacific (De La Fuente et al. 2015), and the northeastern Pacific (Du et al. 2018).

However, the situation in the deglacial western Pacific was more complex. Some studies, based on radiocarbon measurements of paired benthic and planktonic foraminifera in water depths deeper than 2,000 m, indicate that deep-water ventilation in the Pacific has been consistent from the last glacial maximum (LGM) to the present (Broecker et al. 2004, 2008; Lund et al. 2011; Okazaki et al. 2012). This finding challenges the model of ^{14}C-depleted carbon release. Instead, these studies suggest that the Pacific was not a significant carbon reservoir during deglaciation. In contrast, other research presents a different scenario. Okazaki et al. (2010) first reported deep-water formation down to around 3,500 m in the northwestern Pacific during Heinrich Event 1 (H1) (Heinrich 1988), based on radiocarbon data from paired benthic and planktonic foraminifera and global climate model simulations. This process could have facilitated the release of carbon from deep ocean reservoirs. The deep water may have originated from marginal seas, including the Okhotsk and Bering Seas, due to brine rejection, akin to the current formation of North Pacific Intermediate Water (NPIW) (Max et al. 2014). This denser water mass, created by brine rejection, would sink in the east of Japan and spread widely in the northwestern Pacific, primarily along the western boundary of the Pacific basin (Okazaki et al. 2010). Thus, vertical mixing in the North Pacific could release carbon stored in the deep, less-ventilated ocean into the atmosphere (Galbraith et al. 2007; Rae et al. 2014).

Therefore, glacial deep-water circulation in the Pacific was more complex, potentially influenced by two ventilation sources: the global thermohaline circulation path from the North Atlantic and local deep-water formation in the North Pacific. The extent to which these two sources influenced atmospheric carbon dioxide levels during the glacial and deglacial periods remains to be fully understood. To enhance our understanding of carbon storage in the ocean and atmosphere during deglaciation, further research is needed to delineate the distribution and strength of northern-sourced deep water in the Pacific. This study provides a ventilation record from the subtropical western Pacific at a water depth of 2,520 m. The results, given their suitable depth and location, might fill the gap in ventilation records for the subtropical western Pacific from the last glacial maximum to

the present, thereby improving our understanding of the contributions and dominant periods of both southern-sourced and northern-sourced deep water in the western Pacific during the last deglaciation.

2 Regional oceanography

According to modern oceanographic observations and model simulation results, the subsurface and deep water in the Pacific Ocean can be broadly categorized into three layers: the surface and intermediate water (less than 2,000 m), the upper deep layer (2,000–3,500 m), and the lower deep layer (greater than 3,500 m) (Kawabe and Fujio 2010). The water masses in these three layers are ventilated separately by the inflow of Antarctic Intermediate Water (AAIW), Upper Circumpolar Deep Water (UCDW), and Lower Circumpolar Deep Water (LCDW) into the Pacific from the Antarctic Circumpolar Current (ACC). The deep-water circulation in the Pacific is initiated by the sinking of Circumpolar Deep Water (CDW). In the lower deep layer, the northward-moving LCDW eventually upwells to the upper deep layer in the northeastern Pacific, forming the North Pacific Deep Water (NPDW). The NPDW in the upper deep layer then travels southeastward and mixes with the UCDW. This mixture of NPDW and UCDW eventually flows back to the ACC, completing the deep-water circulation in the Pacific. Following the concept of the Great Ocean Conveyor, the deep-water circulation in the Pacific represents the final segment of this conveyor before upwelling into the surface circulation. Therefore, the deep-water masses in the Pacific have older ventilation ages compared to other oceans (Broecker 2010; Kawabe and Fujio 2010).

In the Philippine Sea, the penetration of UCDW into the deep water is limited by oceanic sills with depths of around 3000 m (Kawabe and Fujio 2010). The UCDW, originating from the south, enters the Philippine Sea from the southeast and exits from the northeast (Fig. 1). In this scenario, the deep-water mass in the Philippine Sea is primarily composed of UCDW, with a minor contribution from LCDW (Kawabe and Fujio 2010). Conversely, a recent study based on model results suggests that a portion of NPDW might enter the Philippine Sea through a strong westward current between 10°N and 15°N in the upper deep layer (Zhai and Gu 2020). This finding aligns with observations of chemical tracers in the Pacific. Characterized by high SiO_2 and low dissolved oxygen (DO), the NPDW may mix with UCDW around the Hawaiian Islands (Kawabe and Fujio 2010). The resulting mix of NPDW and UCDW could then enter the Philippine Sea via the northern route along the

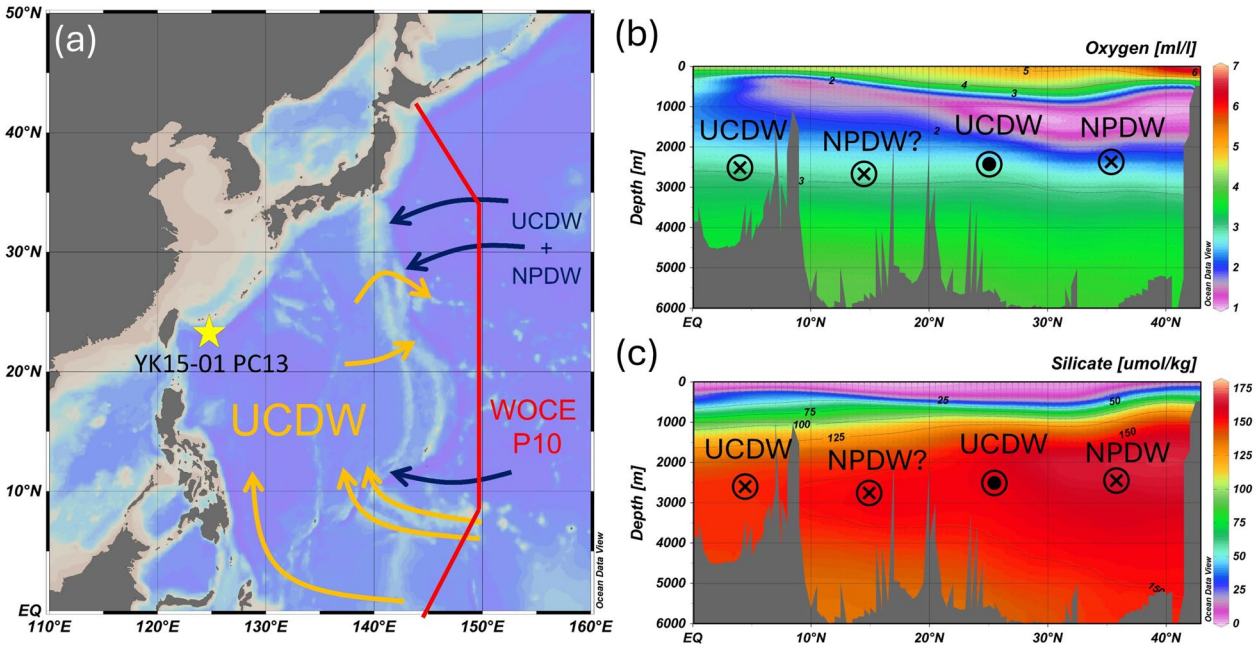

Fig. 1 Regional oceanography in the Philippine Sea. **a**: Yellow star points out the location of core YK15-01 PC13; Orange arrows indicate the path of the Upper Circumpolar Deep Water (UCDW); Deep blue arrows indicate the path of mixed water mass composited of the North Pacific Deep Water (NPDW) and the UCDW. **b** and **c** is the vertical profile of seawater dissolved oxygen and silicate in the WOCE P10 section. Cross symbols indicate the water mass move into the figure and dot symbols indicate the water mass move out of the figure. Regional oceanography is modified from Kawabe and Fujio (2010) and Tian et al. (2021) and the map is created using Ocean Data View. Hydrographic data from Gouretski and Koltermann 2004

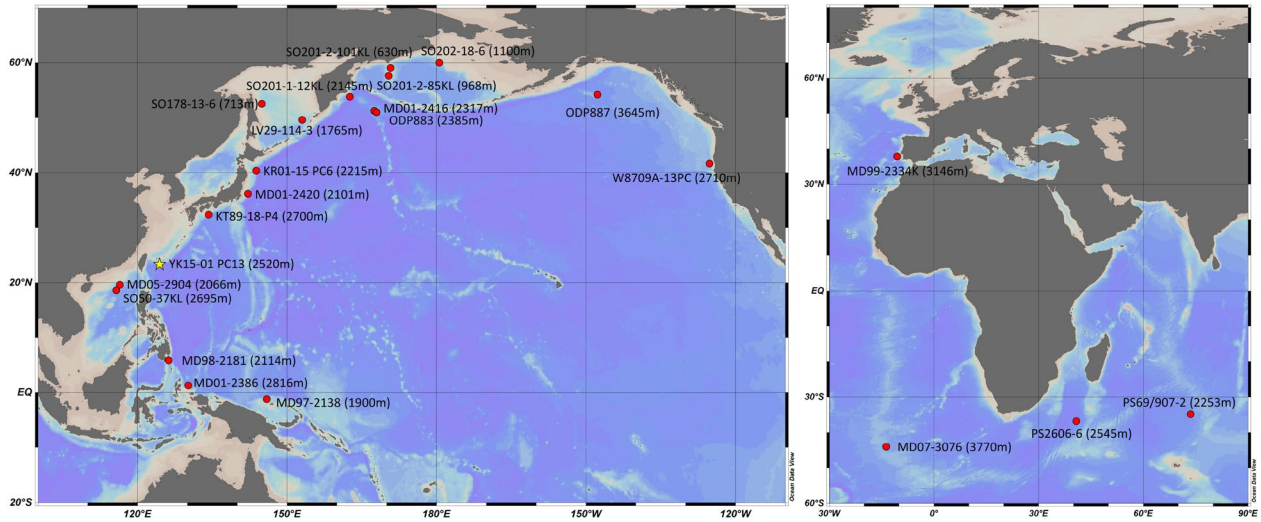

Fig. 2 Locations of core YK15-01 PC13 and references cores used in this study

Izu-Ogasawara Ridge and the southern route at the Yap Mariana Junction (Talley and Joyce 1992; Kaneko et al. 1998, 2001). Based on data from the World Ocean Circulation Experiment (WOCE) Pacific Ocean Atlas (Talley 2007), Tian et al. (2021) concluded that the water mass propagating from the northern path, with lower DO and higher SiO_2, is predominantly influenced by NPDW.

Consequently, while the signatures of the mixed NPDW and UCDW are mainly confined to the northeastern part of the Philippine Sea, the upper deep layer in this region could be influenced by two distinct sources: the younger, southern-sourced UCDW, and the older, northern-sourced mixed deep water (Fig. 1).

3 Materials and methods

The sediment core YK15-01 PC13 (hereafter PC13) for this study was retrieved during the YK15-01 cruise, conducted by the R/V YOKOSUKA at 23.5°N, 124.24°E, from a water depth of 2,520 m in 2015 (Fig. 2). The core's total length is 497 cm. The upper 40 cm of core PC13 features yellowish sediment, transitioning to a grayish color toward the bottom, except for a lighter section between 280 and 380 cm. Two volcanic ash layers are present in core PC13. One layer, found between 380 and 390 cm, is believed to be associated with the Ata tephra (Machida 2002; Kanamatsu et al. 2021). The other ash layer, located at 403 cm, is relatively thin, measuring approximately 1 cm in thickness.

In this study, radiocarbon dating of planktonic foraminifera was used to construct the age model for the core PC13. The difference in radiocarbon dates between coexisting benthic and planktonic foraminifera was employed to calculate the deep-water ventilation age. Six radiocarbon dating points, derived from planktonic foraminifera *Trilobatus sacculifer* (355–500 μm), were previously published by Kanamatsu et al. (2021) and provided by the Japanese Ministry of Education, Culture, Sports, Science, and Technology (MEXT), National Institute of Advanced Industrial Science and Technology. Additional planktonic foraminifera radiocarbon measurements were conducted to enhance the resolution of the age model, and benthic foraminifera were used to determine deep-water ventilation ages. To minimize vital effects across different species, the same species of planktonic foraminifera, *T. sacculifer*, was consistently used, selecting specimens within a size range of 355–500 μm. For benthic foraminifera, specimens of *Cibicidoides wuellerstorfi* and *Uvigerina* spp. larger than 250 μm were chosen. Different species of benthic foraminifera were mixed to meet the minimum sample weight of 4 mg required for radiocarbon measurement. If the total weight was insufficient, shells ranging from 150 to 250 μm were also selected. Mixed samples from adjacent depths were used when the total weight was still too low for radiocarbon testing.

The selected shells were washed with MQ water and soaked overnight in sodium hypochlorite (NaOCl) to remove organic matter, then dried again for further measurement. Radiocarbon measurements were conducted at the NTUAMS Lab, Department of Geosciences, National Taiwan University. To calibrate conventional ^{14}C ages to calendar ages for the age model of core PC13, the Marine20 database (http://claib.org/marine/) was used to obtain the Delta R value. By inputting the location of core PC13, nearly ten reference Delta R values (Hideshima et al., 2001; Yoneda et al., 2007; Hirabayashi et al., 2017)

were utilized, calculating the weighted mean of these ten Delta R values and their standard deviation (Bevington and Robinson, 2003). The conventional ^{14}C ages were then calibrated using Calib 8.2 and Marine20 with a Delta R of -131 ± 98.

The ventilation age of a water mass represents the time elapsed since its last exchange with the atmosphere (Broecker 2010). Different types of water masses, such as subsurface, intermediate, deep, and bottom waters, exhibit varying ventilation ages depending on their circulation and mixing rates with surrounding water masses (Broecker 2010). Since cosmic rays produce radiocarbon on Earth, radiocarbon enters the ocean through the seawater-atmosphere interface, facilitated by biological activities and dissolution effects (Hughen 2007). Therefore, the ^{14}C age of seawater dissolved inorganic carbon (DIC) is a tool for indicating the ventilation age in the ocean. To reconstruct past ventilation ages, coexisting benthic and planktonic foraminifera from the same downcore depths are commonly used, as they preserve the ^{14}C of past seawater DIC (Broecker et al. 1984; Adkins and Boyle 1997; Skinner et al. 2010).

Broecker et al. (1984) suggested that ventilation age can be estimated by subtracting the conventional ^{14}C age of benthic foraminifera from that of planktonic foraminifera (B-P age). Since surface water rapidly exchanges with the atmosphere, the B-P age reflects the age difference between bottom water ^{14}C (i.e., the depth at which benthic foraminifera reside) and the atmosphere. However, this method does not account for varying reservoir ages of surface water, and factors like bioturbation and carbonate dissolution in sediment might influence the B-P age. Adkins and Boyle (1997) introduced the projection age method as an alternative for estimating ventilation age. This approach converts the ^{14}C age of benthic foraminifera into a deep-water $\Delta^{14}C$ value ($\Delta^{14}C$deep-water) and then projected onto the atmospheric $\Delta^{14}C$ curve. It also considers an atmospheric $\Delta^{14}C$ curve based on other radiocarbon measurements, such as from corals or tree rings. The projection age thus means the difference between the calendar age of the $\Delta^{14}C$deep-water point (estimated using coexisting planktonic foraminifera) and the calendar age of the corresponding point on the atmospheric $\Delta^{14}C$ curve, with considering the addition of the surface reservoir age. This method relies on $\Delta^{14}C$ values rather than direct ages, and the errors mainly due to the variations in radiocarbon production and carbon pool exchange rates (Adkins and Boyle 1997), which are common in all ventilation age reconstructions. Another approach, by calculating the difference between benthic ^{14}C and atmospheric ^{14}C ages (B-atm), was proposed by Skinner et al. (2010). This method improves upon the B-P age by subtracting the conventional ^{14}C age of benthic foraminifera from that of planktonic foraminifera and then adding the surface water reservoir age (B−P+R). It addresses the issue in the B-P age where the surface reservoir age is either ignored or assumed constant. The B-atm age thus offers a logic similar to the projection age, representing the difference between the bottom water ^{14}C age and the atmospheric ^{14}C age. While the projection age requires converting the ^{14}C age to $\Delta^{14}C$ values, the B-atm age directly utilizes the ^{14}C age. In the three calculation methods described above, both the projection age and B-atm age use a constant modern estimate of surface reservoir age. The assumption of a fixed surface reservoir age may introduce uncertainty into past ventilation age estimates. In this study, we employed the B-atm age (hereafter referred to as the ventilation age) to reconstruct the ventilation history. In addition to core PC13, reference cores located in the western Pacific (Broecker et al. 2004; Broecker and Barker 2007; Murayama et al. 1992; Minoshima et al. 2007; Du et al., 2018) were used to compare the ventilation ages.

Table 1 Reference surface reservoir ages for B-atm ventilation age calculation. All these data are calculated by referring to the way denoted on Calib program webpage (http://calib.org/marine/) (Reimer and Reimer 2017)

Regions	Data points	Weighted mean *R*	Uncertainty (1σ)
Equatorial to subtropical western Pacific	43	−190	98
Subarctic northwestern Pacific	30	207	177
Southern Ocean (Pacific)	50	−68	85
Northeastern Atlantic	44	−64	148
Southern Ocean (Atlantic)	50	−19	150
Southern Ocean (Indian)	42	−27	115
Northeastern Pacific	50	240	92
South China Sea	14	−158	45

The calendar ages of all reference core data were recalculated using Marine20, following the same protocol as for core PC13. To estimate the surface reservoir age for B-atm age calculations, regional marine reservoir age (ΔR) data from the Marine20 Database were utilized. All core data, including the reference cores and core PC13, were categorized into different regions. To determine the most appropriate surface reservoir age for each region, 50 ΔR values from nearby references were extracted from the Marine20 database. Among these, cores nearby used the same average surface reservoir age, while reference points located in adjacent marginal seas were treated distinctly. For instance, reference data from the South China Sea were not used in estimating the surface reservoir age for the western Pacific region. The selected regions and their corresponding ΔR values are presented in Table 1. The calculated ΔR values were obtained from the Calib program website (http://calib.org/marine/). On the website, regionally weighted ΔR values can be calculated by selecting the appropriate subregion option, and the calculation method can be referenced in Reimer and Reimer (2017).

To verify the feasibility of the mentioned method for better estimating the ventilation age, the youngest B-atm age from core PC13 was calculated and compared with the modern ocean's deep-water radiocarbon age. This comparison utilized data from the WOCE Section P09 in the North Pacific, located at 136.998°E, 20.013°N, at a depth of 2529.2 m, where it is comparable to those of core PC13 for representing of the modern dep-water radiocarbon age of studying area. The $\Delta^{14}C$ value at this WOCE Section point is -231.1 ± 5.9‰. By applying the conversion factor of 8.3 years per 1‰ $\Delta^{14}C$ value (Stuiver et al. 1983), the radiocarbon age difference between deep water and the atmosphere then can be calculated to be 1714.8 ± 50.3 years, and this age means the estimated modern bottom water ventilation age of this region. This calculation uses the modern atmosphere's $\Delta^{14}C$ value of -24.5 ± 1.4‰, as reported in the IntCal20 data (Reimer et al. 2020).

4 Results

The age model for core PC13 was constructed using 12 radiocarbon data points, 2 oxygen isotope stratigraphic tie points, and one ash layer. Of these, six radiocarbon dates were previously published and provided by the Geological Survey of Japan, AIST (Kanamatsu et al. 2021). The remaining six radiocarbon dates were generated in this study. Initially, 13 radiocarbon dating measurements using planktonic foraminifera were made to establish the age model. However, due to a reversal in age between sample A10P and YK15P13-10 (Table 2), where A10P is deeper but older than YK15P13-10, only 12 conventional ages were converted to calendar ages. Given that YK15P13-10 is a published datum, it was used as an age control point instead of A10P.

The age model, spanning from the present to the oldest radiocarbon dating point at 40.16 ka, was interpolated based on the ^{14}C ages. For the period before 40.16 ka, two oxygen isotope stratigraphy correlation points and one published ash layer age were employed to enhance temporal resolution. The oxygen isotope stratigraphy was based on $\Delta^{18}O$ results from four species of planktonic foraminifera, correlating with the SPECMAP planktonic foraminifera oxygen isotope stack curve (Imbrie et al. 1984). Two correlation points were identified during the Marine Isotope Stages (MIS) 5.1 and 5.5, based on the $\Delta^{18}O$ curve features described in Prell et al. (1986), with ages of 80 and 123 ka, respectively. The ash layer, known as Ata tephra, was discussed in a previous study (Machida 2002). Its age, estimated between 105 and 110 ka, corresponds to a layer found across Japan (Machida 2002). Depth-age relationships are presented in Fig. 3, and all age control points are detailed in Table 3.

Figure 6a shows the results of planktonic and benthic conventional radiocarbon age determinations. The oldest planktonic and benthic ages were older than 36 ka, appearing at 170 cm. Two negative B-P ages appeared at 29 and 19 ka (Fig. 4a, b). Since the radiocarbon ages of planktonic and benthic foraminifera indicate the ages of surface and bottom waters, an older bottom water age than surface water is illogical. The negative B-P ages might be caused by picking foraminifera specimens from neighboring depths or by sediment reversal rather than by an actual age difference between planktonic and benthic foraminifera. Additionally, in the deep water $\Delta^{14}C$ data, these two negative B-P age samples had more enriched $\Delta^{14}C$ values than the Marine20 curves (Fig. 4c). The Marine20 data indicate the average surface ocean radiocarbon in the past. Considering the water depth of core PC13 is 2,520 m and the relatively poor deep-water ventilation in this region in the modern ocean, these enriched $\Delta^{14}C$ values cannot be attributed to regional surface ventilation changes or deep-water sinking. Therefore, these two points do not indicate the radiocarbon ages of coexisting surface and bottom seawater and are not appropriate for further ventilation discussions.

Except for the two abnormal values, the ventilation ages of core PC13 rose from around 1,000 years at 40 ka to 2,500 years at 18 ka (during the LGM). After that, ventilation ages decreased to 1,500 years during the cooling event of H1 (Fig. 4b) and rose to 2,500 years again when entering the BA (Hartz and Milthers 1901). Since 15 ka, the ventilation age decreased to more than 1,000 years stably until the end of the YD. After that, the only point

Table 2 Radiocarbon results of core YK15-01 PC13

Smaple ID	Depth (cm)	Foraminifera	Conventional age (yr BP)	Error (1σ)	Calendar Age(yr BP)	Error (1σ)	Lab code
YK15P13-01	0–1.7	*Trilobatus sacculifer*	2220	30	1803	133	Beta-454486
B1	0–4	Mixed benthic	3759	76			NTUAMS-7254
A1P	14–16	*Trilobatus sacculifer*	5488	68	5813	141.5	NTUAMS-7122
A2P	24–26	*Trilobatus sacculifer*	7538	69	7951	134	NTUAMS-7123
YK15P13-06	33.7–35.7	*Trilobatus sacculifer*	10,680	40	12,067	190	Beta-454487
B2	33–36	Mixed benthic	11,705	96			NTUAMS-7255 s
YK15P13-08	37.7–39.7	*Trilobatus sacculifer*	11,040	50	12,534	118.5	Beta-454488
B3	37–40	Mixed benthic	12,354	83			NTUAMS-7256
A3P	44–46	*Trilobatus sacculifer*	12,323	104	13,858	193.5	NTUAMS-7124
A3B	43–46	Mixed benthic	14,163	169			NTUAMS-7131 s
A9P	49–50	*Trilobatus sacculifer*	13,179	91	15,185	195	NTUAMS-7129
A9B	48–51	Mixed benthic	15,427	125			NTUAMS-7252
A4P	59–60	*Trilobatus sacculifer*	14,640	89	17,058	183.5	NTUAMS-7125
A4B	59–60	Mixed benthic	16,094	128			NTUAMS-7132 s
A10P	62–64	*Trilobatus sacculifer*	16,179	101	18,820	165	NTUAMS-7130
A10B	62–64	Mixed benthic	16,097	100			NTUAMS-7253
YK15P13-10	67.7–69.7	*Trilobatus sacculifer*	15,900	50	18,511	157.5	Beta-454489
B4	67–68	Mixed benthic	18,073	361			NTUAMS-7257 s
A5P	79–81	*Trilobatus sacculifer*	18,866	105	22,078	173	NTUAMS-7126
A5B	78–81	Mixed benthic	20,719	187			NTUAMS-7133 s
YK15P13-12	119–121	*Trilobatus sacculifer*	25,170	110	28,675	177	Beta-454490
B5	118–123	Mixed benthic	24,797	169			NTUAMS-7258 s
YK15P13-14	169–171	*Trilobatus sacculifer*	35,940	300	40,164	307.5	Beta-454491
B6	169–171	Mixed benthic	36,639	264			NTUAMS-7259 s

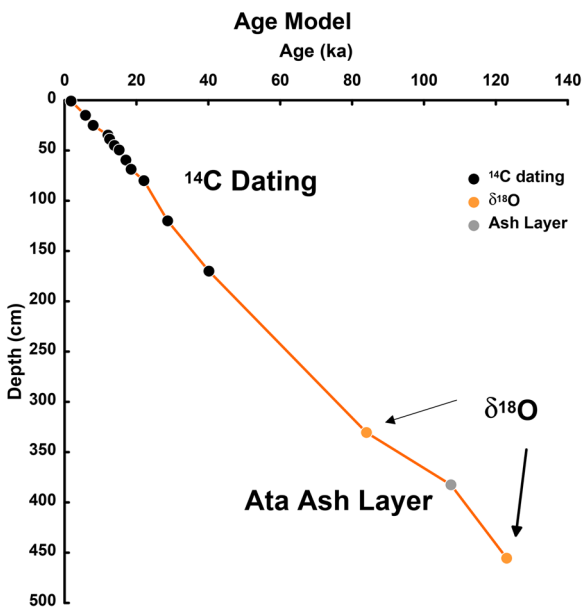

Fig. 3 Age model of core YK15-01 PC13

Table 3 Age control points of core YK15-01 PC13

Depth (cm)	Age (ka)	1σ	Remarks
0–1.7	1.80	0.13	^{14}C
14–16	5.81	0.14	^{14}C
24–26	7.95	0.14	^{14}C
33.7–35.7	12.07	0.19	^{14}C
37.7–39.7	12.53	0.12	^{14}C
44–46	13.86	0.19	^{14}C
49–50	15.19	0.20	^{14}C
59–60	17.06	0.18	^{14}C
67.7–69.7	18.51	0.16	^{14}C
79–81	22.08	0.17	^{14}C
119–121	28.68	0.18	^{14}C
169–171	40.16	0.31	^{14}C
330–331	84.00		^{18}O
378–387	107.50	2.50	Ash layer
455–456	123.00		^{18}O

in the Holocene had a ventilation age of 2,319 years with a dating age of 18 ka (Fig. 4b).

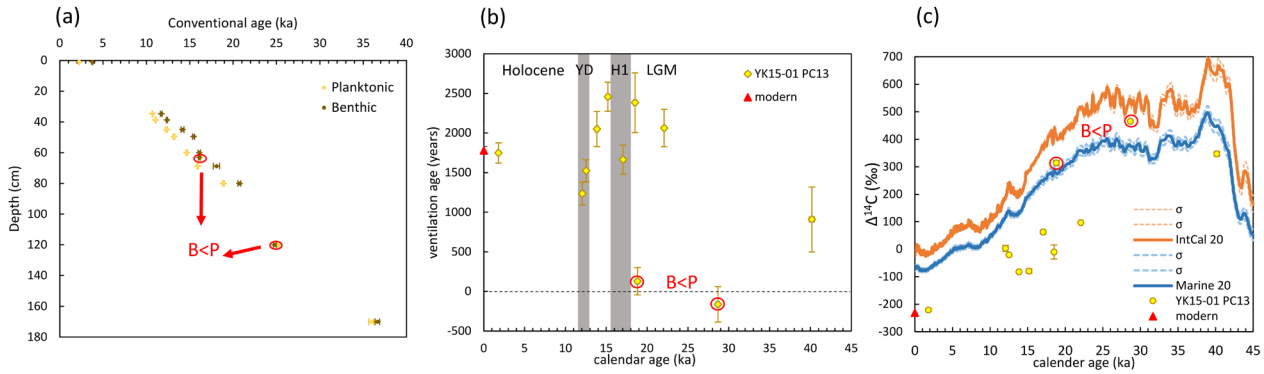

Fig. 4 Ventilation age and ^{14}C values derived from core YK15-01 PC13. **a** Uncorrected conventional age of planktonic and benthic foraminifera. The horizontal difference between the planktonic and benthic foraminifera conventional ages indicates the age difference between the surface and bottom without considering the surface reservoir age. **b** Raw ventilation ages data. Gray squares are H1 and YD during the last deglaciation. The red triangle indicates the modern ventilation age in the western Pacific with a similar water depth to core YK15-01 PC13. **c** Deep-water ^{14}C values. Orange curves and dotted lines indicate the atmosphere ^{14}C from the IntCal 20. Blue curves and dotted lines indicate the surface ocean ^{14}C from the Marine 20 database. The red triangle indicates the modern ^{14}C value. Two circled points are when the benthic conventional age is younger than that of the planktonic conventional age thus creating an extremely low ventilation age value

These results indicate the ventilation age was younger at 40 ka than during and after the LGM. Deep water in the western Pacific might have been better ventilated before the LGM, which was quite different from present conditions. Moreover, ventilation ages decreased significantly and returned to the LGM level throughout the entire BA. This scenario might be explained by the formation of better-ventilated deep water in the northwestern Pacific (Okazaki et al. 2010). If so, the potential deep water in the North Pacific could have spread southward to the subtropical region since core PC13 is further south than previous records that indicated this north-sourced deep water. However, it should be noted that there is only one data point for the ventilation decrease during the YD. After that, ventilation ages decreased steadily from early BA to the middle YD. The amplitude was comparable to that between the YD and the LGM. Since the YD was a cold period similar to H1, the mechanism activating deep-water sinking during H1 might also explain the younger ventilation age during the YD. The ventilation changes and the link could be similar during the two cold events of the last deglaciation.

5 Discussion

5.1 Deep-water ventilation between Western Pacific and Atlantic for the last 45,000 years

In the modern ocean, the sinking of the NADW triggers the AMOC and is considered a driving force of thermohaline circulation, spreading southward to the Southern Ocean (Broecker 2010). In contrast, only intermediate-level water mass sinks in the North Pacific due to insufficient salinity (Talley 1993). Below the intermediate depth, water masses in the North Pacific are composed of the NPDW and the Antarctic Bottom Water (AABW) (Kawabe and Fujio 2010). In this situation, the meridional overturning circulation in the modern Pacific is driven only by the deep water input from the Southern Ocean without a northern deep-water source, resulting in a stronger Atlantic Meridional Overturning Circulation (AMOC) and a weaker Pacific Meridional Overturning Circulation (PMOC) scenario.

However, the glacial Pacific might have had a quite different circulation structure. According to previous studies, the deep-water circulation in the Pacific during the last glacial period had a boundary depth of around 2,000 m, with the water masses above this depth being better ventilated than at present (Herguera et al. 1992; Keigwin 1998; Matsumoto et al. 2002). Combining the records of core PC13 and previous studies in the western Pacific, reconstructed ventilation age records at depths between 2,000 and 3,000 m show an increase of 1,000 years from 40 to 20 ka (Fig. 5). These results support a slowing ventilation scenario when entering the LGM in the western Pacific and are consistent with better-ventilated deep water during the glacial period. However, ventilation ages in the western Pacific had already increased to the Holocene level when entering the LGM (Fig. 5), indicating that a better-ventilated scenario appeared before the LGM, which conflicts with previous results (Herguera et al. 1992; Keigwin 1998; Matsumoto et al. 2002). Furthermore, since no data are available from 30 to 25 ka, the timing of the ventilation transition remains unknown.

During deglaciation, the deep-water ventilation ages in the North Atlantic decreased while the strength of NADW formation increased (Skinner and Shackleton

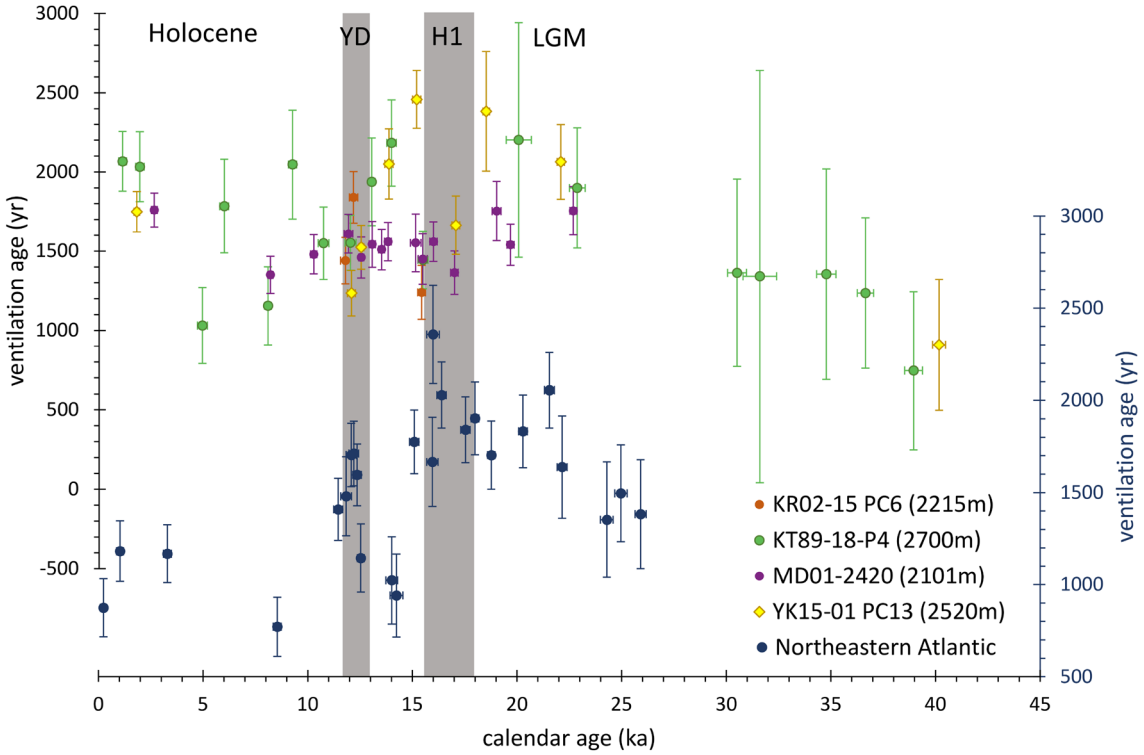

Fig. 5 Ventilation ages calculated from core YK15-01 PC13 and reference core in the western Pacific and northeastern Atlantic. Gray squares are H1 and YD during the last deglaciation

2004). Atlantic ventilation ages started to decrease and then remained around 1,000 years through the Holocene (Fig. 5). Thus, the global deep-water circulation transitioned from a less-ventilated glacial state to a better-ventilated interglacial state. In contrast, the ventilation ages in the western Pacific remained around 2,000 years through the deglaciation and the Holocene, higher than the pre-LGM values of around 1,000 years (Fig. 5). These results indicate opposite deep-water circulation changes between the Pacific and the Atlantic from the last glacial period to the interglacial period. Moreover, such opposite ventilation change patterns also appeared during the two deglacial cold events. While ventilation ages decreased significantly in the western Pacific, ventilation ages in the Atlantic increased markedly and returned to Holocene levels after the end of H1 and YD.

Such inverted ventilation records in the deep Pacific and Atlantic could be linked to the Atlantic–Pacific seesaw during glacial to interglacial cycles. Using model simulation results, Saenko et al. (2004) investigated the connection between the meridional overturnings circulations (AMOC and PMOC) and climate variability between the Atlantic and the Pacific. The AMOC and PMOC exhibit a seesaw behavior where freshwater input into the Atlantic weakens the AMOC due to reduced salinity and inhibits deep water formation, while freshwater removal in the North Pacific allows for denser, colder water to sink, thus enhancing the PMOC. This seesaw pattern is influenced by factors such as the closure of the Bering Strait during the glacial period, which prevents the transfer of freshwater perturbations between the North Atlantic and Pacific (Saenko et al. 2004; Hu et al. 2012).

The results of this study support a seesaw-like scenario between the glacial and interglacial periods, particularly highlighting an enhanced PMOC during H1, as proposed by Okazaki et al. (2010). Furthermore, combining ventilation records from the western Pacific and North Atlantic reveals a long-term reversal pattern from the last glacial period to the Holocene. This phenomenon suggests two timescales of the Atlantic and Pacific seesaw: one at the millennial scale, observed in events like H1 and YD, and another at the glacial to interglacial cycles, spanning approximately 100 thousand years. While the former is supported by previous studies using proxies and models, additional data are needed to further validate and elucidate the long-term seesaw relationship between the AMOC and PMOC.

5.2 Better ventilation events during Heinrich event 1 and younger dryers

During deglaciation, ventilation ages in the western Pacific decreased by approximately 1,000 years during H1 and YD, respectively (Fig. 6c). Since there was no deep-water formation in the western Pacific (Kawabe and Fujio 2010), these better ventilation events could have been contributed by water masses ventilating from high-latitude areas. One possible source could have been the deep-water formation in the North Pacific. Previous studies in the North Pacific, based on sediment proxies and earth system models, have shown that an enhanced NPIW or glacial North Pacific Deep Water (NPDW) formed with potential depths of up to 3,000 m during H1 and YD (Okazaki et al. 2010; Rae et al. 2014). This glacial NPDW could have been caused by the breakdown of density stratification in the North Pacific and had the potential to release deep-stored carbon from the deep ocean reservoir, contributing to the rise in atmospheric CO_2 during deglaciation (Rae et al. 2014). This better-ventilated water mass mainly spread along the western Pacific boundary and could have reached sites in the mid-low-latitude areas (Okazaki et al. 2010).

To verify if this north-sourced water was responsible for the better ventilation events, ventilation age records from potential source areas of glacial NPDW, such as the Sea of Okhotsk and the Bering Sea (Max et al. 2014), were compared in this study. Ventilation ages from the Sea of Okhotsk and the Bering Sea decreased significantly during the middle of H1 (Heinrich 1988) (Fig. 6a). The magnitude of ventilation age decrease in the source area was approximately 1,500 years, longer than the around 1,000 years observed in downstream sites (Fig. 6a). Since the water mass could mix with surrounding water masses during transport, ventilation conditions in downstream sites might have been more consistently than in the source region. However, the difference of 500 years between the high-latitude source region and the low-latitude downstream region is significantly larger than present-day differences (Talley 2007). If this reconstruction is accurate, the gradient of ventilation age from high latitude to subtropical regions during this period was larger than it is today.

Moreover, the initiation of ventilation age decrease in high latitudes occurred in the middle of H1, slightly later than in mid and low latitudes (Fig. 6a, c). If the north-sourced water was indeed the main source, the initial timing of ventilation age decrease in the source region should have been earlier or roughly simultaneous with downstream sites, considering potential age model errors. However, this discrepancy could also be due to the lack of data points during the early H1 in low-latitude records (Fig. 6c).

On the other hand, in the far northwestern Pacific at depths deeper than 2,145 m, which is beyond the Sea of Okhotsk and Bering Sea and a potential area of denser water sinking in the Pacific (Yasuda 1997), ventilation ages decreased by more than 1,000 years from early H1 to the end of YD (Fig. 6b) and did not correlate with signals in shallower waters. These deeper water records support that enhanced NPIW was constrained to depths above approximately 2,000 m, rather than deeper depths up to 3,000 m as observed in the high-latitude source region (Max et al. 2014).

Another possible source of better-ventilated deep water in the western Pacific during H1 and YD could be deep-water ventilation originating from the Southern Ocean. Modern oceanographic observations indicate that water masses deeper than 2,000 m in the western Pacific are composed of Upper Circumpolar Deep Water (UCDW), sourced from the Southern Ocean, which flows northward along the island arcs in the western Pacific toward lower latitude areas (Kawabe and Fujio 2010). The UCDW continues to flow northward to around 30°N before mixing with north-sourced North Pacific Deep Water (NPDW) and changing direction to flow eastward (Kaneko et al. 2001; Kawabe and Fujio 2010).

Similar ventilation age decreases during H1 can be observed in the Southern Ocean, although these are relatively minor (Ronge et al. 2020) (Fig. 6g). Long-term ventilation changes in the Southern Ocean follow patterns similar to those in the Atlantic, with stable decreases from the last glacial periods to the Holocene. During H1, ventilation age decreased slightly in the Indian sector of the Southern Ocean, although records from the middle of H1 are lacking. The tropical Pacific deep-water circulation change connected to the south-sourced water is also supported from the water temperature signals (Stott et al. 2007). If better-ventilated water originates from the south, similar signals should be recorded along its transport path. However, previous studies in the western Pacific have shown consistent ventilation changes since the last glacial periods, suggesting no significant changes in deep-water ventilation or release of deep carbon (Broecker et al. 2004, 2008; Okazaki et al. 2012) (Fig. 6e). Another study partially attributed the presence of better-ventilated water in the northern South China Sea (SCS) to potentially enhanced NPIW during H1 and YD (Wan and Jian 2014). However, given that the amplitude of ventilation age decrease is considerably higher in the northwestern Pacific, it is not sufficient to infer that better-ventilated deep water in the Pacific was distributed to regions outside of the SCS during the last glacial period (Fig. 6d).

Considering the amplitude and pattern of ventilation age changes, it is plausible that the two younger

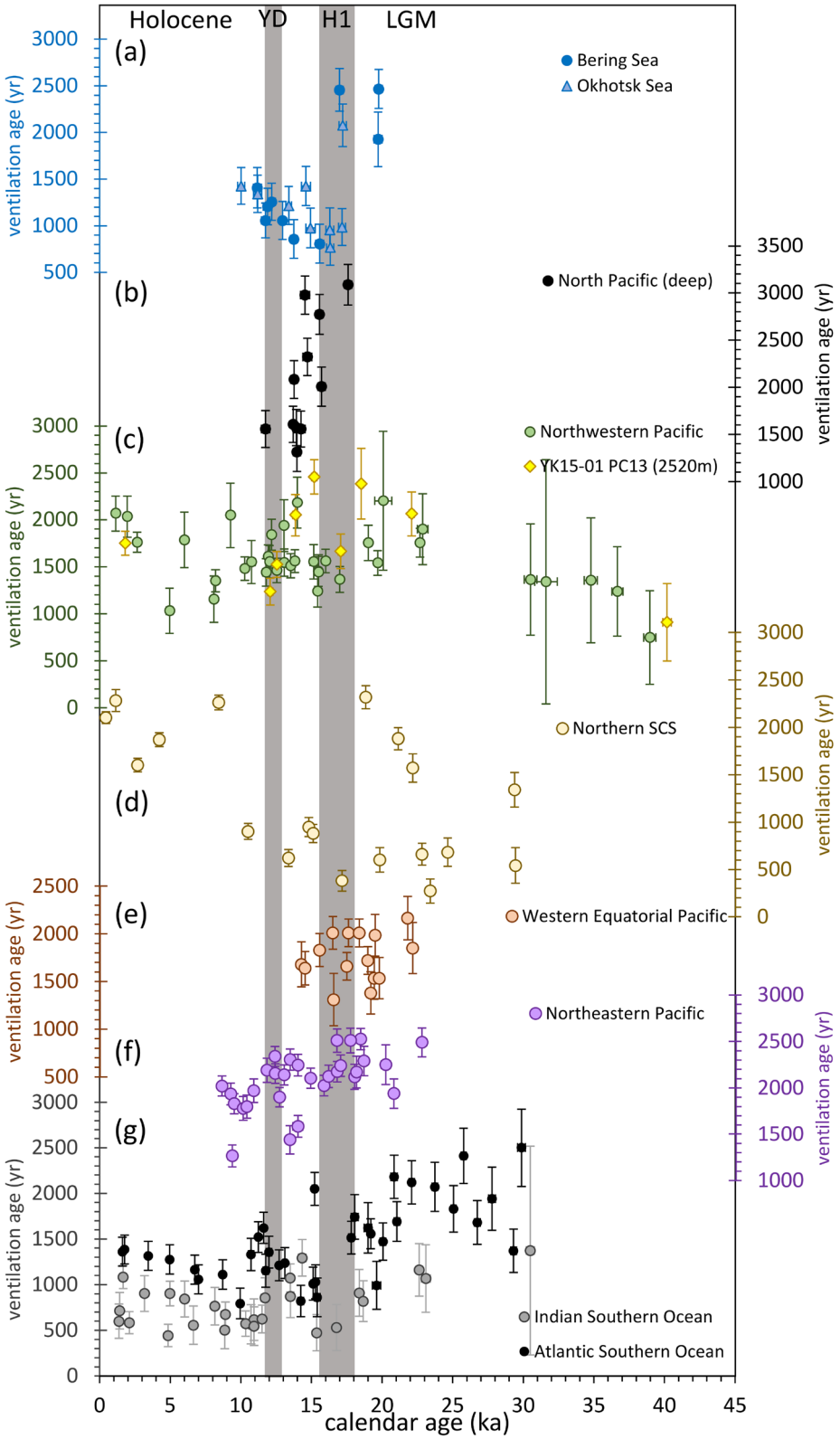

Fig. 6 Ventilation ages calculated from **a** the Bering Sea and Okhotsk Sea (Max et al. 2014); **b** subarctic northwestern Pacific (Max et al. 2014; Sarnthein et al. 2006); **c** YK15-01 PC13 and northwestern Pacific (mid-latitude) (this study; Murayama et al. 1992; Minoshima et al. 2007; Okazaki et al. 2012); **d** northern South China Sea (Wan and Jian 2014); **e** western equatorial Pacific (Broecker et al. 2004, 2007); **f** northeastern Pacific (Galbraith et al. 2007; Lund et al. 2011); **g** Southern Ocean (Ronge et al. 2020; Skinner et al. 2010). Gray squares are H1 and YD during the last deglaciation

ventilation age events in the subtropical western Pacific were contributed by better-ventilated water originating from the northern source rather than the southern source. The water depth of each record indicates that this younger water could sink to depths greater than 2,500 m in downstream sites, which is even deeper than the source region (Max et al. 2014) (Fig. 6a, b, c). Thus, better-ventilated water from the North Pacific could have distributed southward to the western subtropical region at depths of around 2,500 m (this study), but not to the equatorial region (Broecker et al. 2004, 2008). Furthermore, additional proxies and mechanisms are necessary to confirm whether the better-ventilated layer was shallower in the high-latitude region compared to downstream sites.

Compared to the western Pacific, ventilation changes were more stable and slightly older during H1 and YD in the eastern Pacific (Galbraith et al. 2007; Lund et al. 2011) (Fig. 6f). Model simulations of enhanced NPIW during H1, as discussed by Okazaki et al. (2010), indicated that better-ventilated water was primarily distributed in the western Pacific, spreading from northwestern to southeastern regions. Consequently, the northeastern Pacific is positioned downstream relative to the deep-water ventilation during deglacial periods and received minimal or no signals of younger water. Studies in the northeastern Pacific have indeed found it to be predominantly occupied by older water masses (Galbraith et al. 2007; Lund et al. 2011). The long-term pattern of ventilation changes in the northeastern Pacific mirrors that of the Atlantic, contrasting with the western Pacific (Fig. 5, 6f).

In summary, deep-water ventilation in the subtropical northwestern Pacific was enhanced during H1 and YD, likely ventilated through an intensified NPIW in the northwestern Pacific rather than originating from the Southern Ocean. Furthermore, the western and eastern Pacific exhibit distinct scenarios: the western Pacific tracks changes in the strength of deep-water formation in the north, while the eastern Pacific aligns more closely with the Atlantic and the covariant content of the Atlantic Meridional Overturning Circulation (AMOC). This disparity not only underscores different ventilation sources between the western and eastern Pacific but also informs potential distributions of deep-water formation during deglacial periods in the Pacific Ocean.

6 Conclusions

In this study, radiocarbon-derived ventilation ages were utilized to reconstruct deep-water circulation in the subtropical western Pacific. Ventilation age patterns differed between the Atlantic and the Pacific since the last glacial maximum (LGM), suggesting a seesaw-like oscillation during millennial-scale and glacial to interglacial cycles. Additionally, two episodes of improved ventilation during Heinrich Event 1 (H1) and the Younger Dryas (YD) may be attributable to northern-sourced deep-water rather than southern-sourced Upper Circumpolar Deep Water (UCDW), as evidenced by the absence of similar records along the path from the southern source.

Conversely, records from the eastern Pacific displayed an opposite pattern compared to those in the western Pacific and resembled patterns observed in the Atlantic. By integrating records from the western Pacific, eastern Pacific, Southern Ocean, and Atlantic, these findings support the hypothesis of deep-water formation in the North Pacific during glacial and deglacial periods, thereby refining our understanding of the distribution of such better-ventilated water during deglaciation in the northwestern Pacific.

Supplementary Information

The online version contains supplementary material available at https://doi.org/10.1186/s40645-024-00675-2.

Additional file1 (XLSX 24 KB)

Acknowledgements

This research was supported by the National Science Council (NSTC 109-2116-M-110 -002-, 110-2116-M-110-001- and 111-2811-M-110-028-), National Taiwan Normal University, and National Sun Yat sen-University. We express our sincere thanks to the funding support by the Japanese Ministry of Education, Culture, Sports, Science, and Technology (MEXT) Project and Japan Agency for Marine Science and Technology (JAMSTEC), which offer sediment samples, and the staffs who helped the samples processing. The captains. officers, crews and marine technicians in the R/Vs Yokosuka are appreciated for their efforts during the data collection. We also thank the helps from the NTUAMS ^{14}C dating Lab for processing foraminiferal samples.

Author contributions

The individual contributions of authors to the manuscript should be specified in this section. The authors should be referred to by their initials. Y.P. Chang, H.L. Lin, and W.C. Hsiung proposed the topic and conceived and designed the study. K. Ikehara and T. Kanamatsu worked during the cruise and obtained the sediment core. H.S. Mii helped analyze the isotope. All authors read and approved the final manuscript.

Funding

This research was supported by the National Science Council (NSTC 109–2116-M-110 -002-, 110–2116-M-110–001- and 111–2811-M-110–028-).

Availability of data and material

The datasets supporting the conclusions of this article are included within the article and its additional files.

Declarations

Competing interests

The authors declare that they have no competing interest.

Author details

[1]Department of Earth and Planetary Sciences, Kyushu University, 744 Motooka Nishi-Ku, Fukuoka 819-0395, Japan. [2]Department of Oceanography, National Sun Yat-sen University, No.70 Lien-Hai Rd., Kaohsiung 804, Taiwan, Republic of China. [3]Sustainable Ocean Governance Center, National Sun Yat-sen University, No.70 Lien-Hai Road, Kaohsiung 804, Taiwan, Republic of China. [4]Department of Earth Sciences, National Taiwan Normal University, No. 88, Sec. 4, Tingzhou Rd., Taipei City 116, Taiwan, Republic of China. [5]Geological Survey

of Japan, National Institute of Advanced Industrial Science and Technology, Central 7, 1-1-1 Higashi, Tsukuba, Ibaraki 305-8567, Japan. [6]Japan Agency for Marine-Earth Science and Technology, 2-15 Natsushima-Cho, Yokosuka, Kanagawa 237-0061, Japan.

Received: 15 July 2024 Accepted: 15 December 2024
Published online: 06 January 2025

References

Adkins JF, Boyle EA (1997) Changing atmospheric $\Delta^{14}C$ and the record of deep water paleoventilation ages. Paleoceanography 12:337–344

Anderson R, Ali S, Bradtmiller L, Nielsen S, Fleisher M, Anderson B, Burckle L (2009) Wind-driven upwelling in the Southern Ocean and the deglacial rise in atmospheric CO_2. Science 323:1443–1448

Beck JW, Richards DA, Lawrence R, Silverman BW, Smart PL, Donahue DJ, Hererra-Osterheld S, Burr GS, Calsoyas L, Timothy A (2001) Extremely large variations of atmospheric ^{14}C concentration during the last glacial period. Science 292:2453–2458

Broecker W (2010) The Great Ocean Conveyor. Princeton University Press, Princeton

Broecker W, Barker S (2007) A 190‰ drop in atmosphere's ^{14}C during the "Mystery Interval"(17.5–14.5 kyr). Earth Planet Sci Lett 256:90–99

Broecker W, Mix A, Andree M, Oeschger H (1984) Radiocarbon measurements on coexisting benthic and planktic foraminifera shells: potential for reconstructing ocean ventilation times over the past 20000 years. Nucl Instrum Methods Phys Res Sect B 5:331–339

Broecker W, Barker S, Clark E, Hajdas I, Bonani G, Stott L (2004) Ventilation of the glacial deep Pacific Ocean. Science 306:1169–1172

Broecker W, Clark E, Barker S (2008) Near constancy of the Pacific Ocean surface to mid-depth radiocarbon-age difference over the last 20 kyr. Earth Planet Sci Lett 274:322–326

De La Fuente M, Skinner L, Calvo E, Pelejero C, Cacho I (2015) Increased reservoir ages and poorly ventilated deep waters inferred in the glacial Eastern Equatorial Pacific. Nat Commun 6:1–11

Du J, Haley BA, Mix AC, Walczak MH, Praetorius SK (2018) Flushing of the deep Pacific Ocean and the deglacial rise of atmospheric CO_2 concentrations. Nat Geosci 11:749–755

Fairbanks RG, Mortlock RA, Chiu T-C, Cao L, Kaplan A, Guilderson TP, Fairbanks TW, Bloom AL, Grootes PM, Nadeau M-J (2005) Radiocarbon calibration curve spanning 0–50,000 years BP based on paired $^{230}Th/^{234}U/^{238}U$ and ^{14}C dates on pristine corals. Quatern Sci Rev 24:1781–1796

Galbraith ED, Jaccard SL, Pedersen TF, Sigman DM, Haug GH, Cook M, Southon JR, Francois R (2007) Carbon dioxide release from the North Pacific abyss during the last deglaciation. Nature 449:890–893

Gouretski V, Koltermann KP (2004) WOCE global hydrographic climatology. Berichte des BSH 35:1–52

Hartz N, & Milthers V (1901) Det senglaciale ler i Allerød Teglværksgrav

Heinrich H (1988) Origin and consequences of cyclic ice rafting in the northeast Atlantic Ocean during the past 130,000 years. Quatern Res 29:142–152

Herguera J, Jansen E, Berger W (1992) Evidence for a bathyal front at 2000 M depth in the glacial Pacific, based on a depth transect on Ontong Java Plateau. Paleoceanography 7:273–288

Hideshima S, Matsumoto E, Abe O, Kitagawa H (2001) Northwest pacific marine reservoir correction estimated from annually banded coral from Ishigaki Island, Southern Japan. Radiocarbon 43:473-476

Hirabayashi S, Yokoyama Y, Suzuki A, Miyairi Y, Aze T (2017) Short-term fluctuations in regional radiocarbon reservoir age recorded in coral skeletons from the Ryukyu Islands in the north-western Pacific. J Quatern Sci 32:1-6

Hu A, Meehl GA, Han W, Abe-Ouchi A, Morrill C, Okazaki Y, Chikamoto MO (2012) The Pacific-Atlantic seesaw and the Bering Strait. Geophys Res Lett. https://doi.org/10.1029/2011GL050567

Hughen KA (2007) Chapter five radiocarbon dating of deep-sea sediments. Dev Mar Geol 1:185–210

Hughen K, Lehman S, Southon J, Overpeck J, Marchal O, Herring C, Turnbull J (2004) ^{14}C activity and global carbon cycle changes over the past 50,000 years. Science 303:202–207

Imbrie J, Hays JD, Martinson DG, McIntyre A, Mix AC, Morley JJ, Pisias NG, Prell WL, Shackleton NJ (1984) The orbital theory of Pleistocene climate: support from a revised chronology of the marine $\delta^{18}O$ record

Kanamatsu T, Ikehara K, Misawa A (2021) Seafloor morphology and sediment magnetic fabric in a putative 1771 Meiwa tsunami source region in the southern Ryukyu Islands, SW Japan. Geol Soc Lond Spec Publ 501:289–299

Kaneko I, Takatsuki Y, Kamiya H, Kawae S (1998) Water property and current distributions along the WHP-P9 section (137°–142°) in the western North Pacific. J Geophys Res Oceans 103:12959–12984

Kaneko I, Takatsuki Y, Kamiya H (2001) Circulation of intermediate and deep waters in the Philippine Sea. J Oceanogr 57:397–420

Kawabe M, Fujio S (2010) Pacific Ocean circulation based on observation. J Oceanogr 66:389–403

Keigwin LD (1998) Glacial-age hydrography of the far northwest Pacific Ocean. Paleoceanography 13:323–339

Khatiwala S, Primeau F, Holzer M (2012) Ventilation of the deep ocean constrained with tracer observations and implications for radiocarbon estimates of ideal mean age. Earth Planet Sci Lett 325:116–125

Lund DC, Mix AC, Southon J (2011) Increased ventilation age of the deep northeast Pacific Ocean during the last deglaciation. Nat Geosci 4:771–774

Machida H (2002) Volcanoes and tephras in the Japan area. Glob Environ Res-English Ed 6:19–28

Matsumoto K, Oba T, Lynch-Stieglitz J, Yamamoto H (2002) Interior hydrography and circulation of the glacial Pacific Ocean. Quatern Sci Rev 21:1693–1704

Max L, Lembke-Jene L, Riethdorf J-R, Tiedemann R, Nürnberg D, Kühn H, Mackensen A (2014) Pulses of enhanced North Pacific Intermediate Water ventilation from the Okhotsk Sea and Bering Sea during the last deglaciation. Clim past 10:591–605

Minoshima K, Kawahata H, Irino T, Ikehara K, Aoki K, Uchida M, Yoneda M, Shibata Y (2007) Deep water ventilation in the northwestern North Pacific during the last deglaciation and the early Holocene (15–5 cal. kyr BP) based on AMS ^{14}C dating. Nucl Instrum Methods Phys Res Sect B 259:448–452

Monnin E, Indermuhle A, Dallenbach A, Fluckiger J, Stauffer B, Stocker TF, Raynaud D, Barnola J-M (2001) Atmospheric CO_2 concentrations over the last glacial termination. Science 291:112–114

Murayama M, Taira A, Iwakura H, Matsumoto E, Nakamura T (1992) Northwest Pacific deep water ventilation rate during the past 35,000 years with the AMS ^{14}C foraminifera ages. Summaries of Researchers Using AMS at Nagoya University (Nagoya University Center for Chronological Research), 114–121

Negre C, Zahn R, Thomas AL, Masque P, Henderson GM, Martinez-Mendez G, Hall IR, Mas JL (2010) Reversed flow of Atlantic deep water during the last glacial maximum. Nature 468:84–88

Okazaki Y, Timmermann A, Menviel L, Harada N, Abe-Ouchi A, Chikamoto M, Mouchet A, Asahi H (2010) Deepwater formation in the North Pacific during the last glacial termination. Science 329:200–204

Okazaki Y, Sagawa T, Asahi H, Horikawa K, Onodera J (2012) Ventilation changes in the western North Pacific since the last glacial period. Clim past 8:17–24

Prell WL, Imbrie J, Martinson DG, Morley JJ, Pisias NG, Shackleton NJ, Streeter HF (1986) Graphic correlation of oxygen isotope stratigraphy application to the late Quaternary. Paleoceanography 1:137–162

Rae JW, Sarnthein M, Foster GL, Ridgwell A, Grootes PM, Elliott T (2014) Deep water formation in the North Pacific and deglacial CO_2 rise. Paleoceanography 29:645–667

Reimer RW, Reimer PJ (2017) An Online Application for R Calculation. Radiocarbon 59:1623–1627

Reimer PJ, Austin WE, Bard E, Bayliss A, Blackwell PG, Ramsey CB, Butzin M, Cheng H, Edwards RL, Friedrich M (2020) The IntCal20 Northern Hemisphere radiocarbon age calibration curve (0–55 cal kBP). Radiocarbon 62:725–757

Ronge TA, Prange M, Mollenhauer G, Ellinghausen M, Kuhn G, Tiedemann R (2020) Radiocarbon evidence for the contribution of the Southern Indian Ocean to the evolution of atmospheric CO_2 over the last 32,000 years. Paleoceanogr Paleoclimatol. https://doi.org/10.1029/2019PA003733

Saenko OA, Schmittner A, Weaver AJ (2004) The Atlantic-Pacific seesaw. J Clim 17:2033–2038

Sarnthein M, Kiefer T, Grootes PM, Elderfield H, Erlenkeuser H (2006) Warmings in the far northwestern Pacific promoted pre-Clovis immigration to America during Heinrich event 1. Geology 34:141–144
Sigman DM, Hain MP, Haug GH (2010) The polar ocean and glacial cycles in atmospheric CO_2 concentration. Nature 466:47–55
Skinner L, Shackleton N (2004) Rapid transient changes in northeast Atlantic deep water ventilation age across Termination I. Paleoceanograph. https://doi.org/10.1029/2003PA000983
Skinner LC, Fallon S, Waelbroeck C, Michel E, Barker S (2010) Ventilation of the deep Southern Ocean and deglacial CO_2 rise. Science 328:1147–1151
Stott L, Timmermann A, Thunell R (2007) Southern hemisphere and deep-sea warming led deglacial atmospheric CO_2 rise and tropical warming. Science 318:435–438
Stuiver M, Quay PD, Ostlund H (1983) Abyssal water carbon-14 distribution and the age of the world oceans. Science 219:849–851
Talley LD (1993) Distribution and formation of North Pacific intermediate water. J Phys Oceanogr 23:517–517
Talley LD (2013) Closure of the global overturning circulation through the Indian, Pacific, and Southern Oceans: schematics and transports. Oceanography 26:80–97
Talley LD, Joyce TM (1992) The double silica maximum in the North Pacific. J Geophys Res: Oceans 97:5465–5480
Talley LD (2007) Hydrographic Atlas of the World Ocean Circulation Experiment (WOCE) Volume 2: Pacific Ocean. WOCE International Project Office Southampton
Tian Z, Zhou C, Xiao X, Wang T, Qu T, Yang Q, Zhao W, Tian J (2021) Water-mass properties and circulation in the deep and abyssal Philippine Sea. J Geophys Res: Oceans. https://doi.org/10.1029/2020JC016994
Wan S, Jian Z (2014) Deep water exchanges between the South China Sea and the Pacific since the last glacial period. Paleoceanography 29:1162–1178
Yasuda I (1997) The origin of the North Pacific intermediate water. J Geophys Res: Oceans 102:893–909
Yoneda M, Uno H, Shibata Y, Suzuki R, Kumamoto Y, Yoshida K, Sasaki T, Suzuki A, Kawahata H (2007) Radiocarbon marine reservoir ages in the western Pacific estimated by pre-bomb molluscan shells. Nucl Instrum Meth Phys Res Sect B: Beam Inter Mater Atom 259:432–437
Zhai F, Gu Y (2020) Abyssal circulation in the Philippine Sea. J Ocean Univ China 19:249–262

Publisher's Note